Smart Rock Technology for Real-time Monitoring of Bridge Scour and Riprap Effectiveness – Design Guidelines and Visualization Tools (Progress Report No. 3)

Contract No: OASRTRS-14-H-MST
(Missouri University of Science and Technology)

Reporting Period: April 1 – June 30, 2015

PI: Genda Chen

Program Manager: Mr. Caesar Singh

Submission Date: July 15, 2015

TABLE OF CONTENTS

EXECUTIVE SUMMARY

In the third quarter of this project, the first attempt for field measurement with an automatically pointing-up system (APUS) was carried out. The prototype smart rock was prepared with a cylindrical rare earth permanent magnet oriented upward based on gravity. It was placed around a bridge pier to generate a perturbation to the surrounding magnetic field. The perturbation was measured for the localization of the magnet. A modular wood frame that supports two magnetometer sensors in field applications was designed and built to enable the magnetic field measurement at various elevations and horizontal distances. The wood frame was used at one bridge site to measure a spatial distribution of the magnetic field. It is simple and easy to assemble with plastic screws. However, it was observed from the field test that, due to its flexibility, the wood frame swung appreciably even at low wind velocity and thus the sensor measurement was not as repeatable as expected. Therefore, a more rigid yet light frame made of aluminum and fiber reinforced polymer materials was designed and currently under fabrication.

Updated hydraulic data sets at the Highway 9 Bridge over Kings Creek were obtained from the California Department of Transportation. They were used to revise the design of smart rocks. To increase the measurement distance, a smart rock with two magnets (each being the same as previously used with 4" in diameter and 2" in height) or one larger magnet (6" in diameter and 2" in thickness) is being designed. The plan for the field deployment of smart rocks at four bridge sites was developed.

Magnetometer G858 measures the intensity of a magnetic field only without knowing its polarization direction. To improve the accuracy of smart rock localization at bridge sites, a 3-axis flux magnetometer was ordered for future field measurement. The new magnetometer also adds the capability for graphical display of the measured data during tests, which allows data quality check in real time.

In addition, a deployment plan of smart rocks at four bridge sites has been developed during this quarter.

I - TECHNICAL STATUS

I.1 ACCOMPLISHMENTS BY MILESTONE

In this quarter, a mock-up test on the deck of US63 Bridge over the Gasconade River was conducted with a smart rock prototype using an automatically pointing-up system (APUS) placed on the ground near the bridge pier. The two sensors of Magnetometer 858 were mounted on the wood frame that was placed outside the bridge railing and extended downward from the bridge deck. For each measurement, the coordinates of the two sensors were determined from a total station set in a nearby reference station. The final size and configuration of smart rocks were modified based on the updated hydraulic data recently made available and based on the expected longer measurement distance. In addition, a rigid yet light modular frame to support the magnetometer sensors in field tests was designed and under fabrication based on the field test at the US63 Bridge. To further improve the accuracy of smart rock localization, a 3-axis fluxgate magnetometer was ordered to measure both the intensity and orientation of a magnet.

Task 1.1 Motion of Smart Rocks under Various Flow Conditions - Critical Flow Conditions Summarized for Various Cases

A. Incipient Motion at Highway 9 over Kings Creek (Bridge No.36-0054)

As shown in Figure 1, the Kings Creek Bridge is a 2-span structure that carries Highway 9 traffic in Santa Cruz County over the Kings Creek. It is located at the apex of a bend in the channel with the main channel flowing under Span 2.

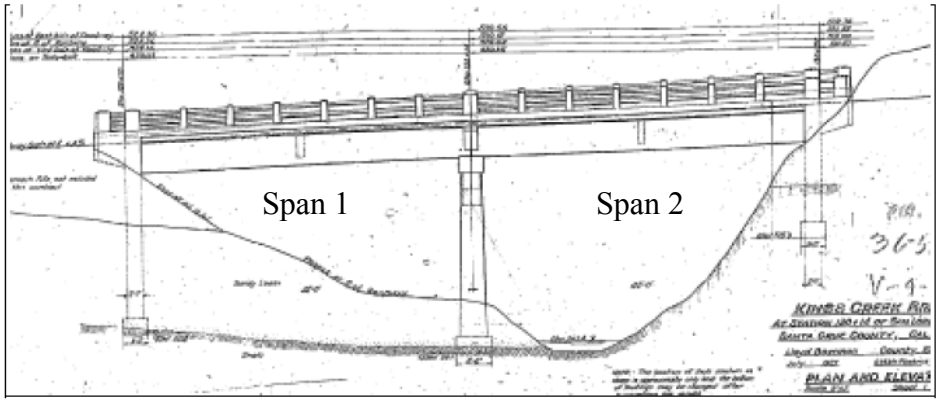

Figure 1 Schematic View of Kings Creek Bridge No.36-0054

This bridge was classified as scour critical in 2004; its foundations were determined to be unstable for assessed or calculated scour conditions. The footing pads at Bent 2 for both columns were found to be severely exposed. In addition to the exposure of the bent footings, a large section of the downstream right bank (looking in the downstream direction) near the bridge is severely eroded. In order to assess the scour condition, a 2D hydraulic model of the flow around the bend where the bridge crossing is located was established and analyzed by Caltrans to determine various hydraulic parameters at the bridge site.

The 100-year flood discharge (Q_{100}) was estimated to be 76.693 m^3/s using STREAMSTATS, a web-based program developed by the USGS. The distribution of the averaged flow velocity over depth and the flow depth analyzed from SRH-2D run corresponding to the 100-year flood were provided by Caltrans as shown in Figures 2 and 3.

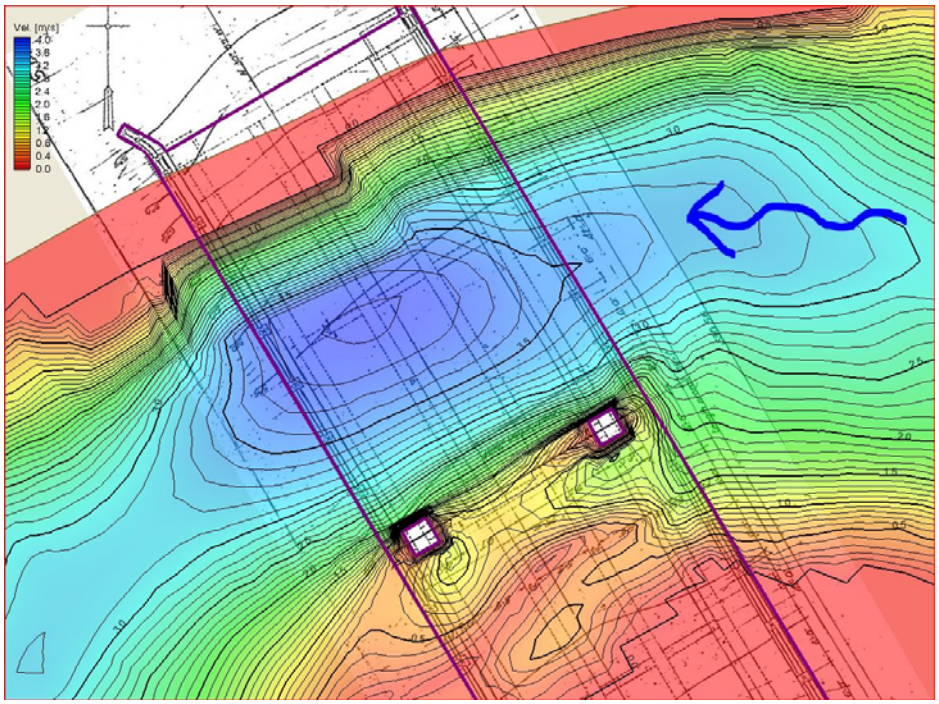

Figure 2 Depth-averaged Velocity Contours for the Q100 @ Kings Creek (Br. 36-0054)

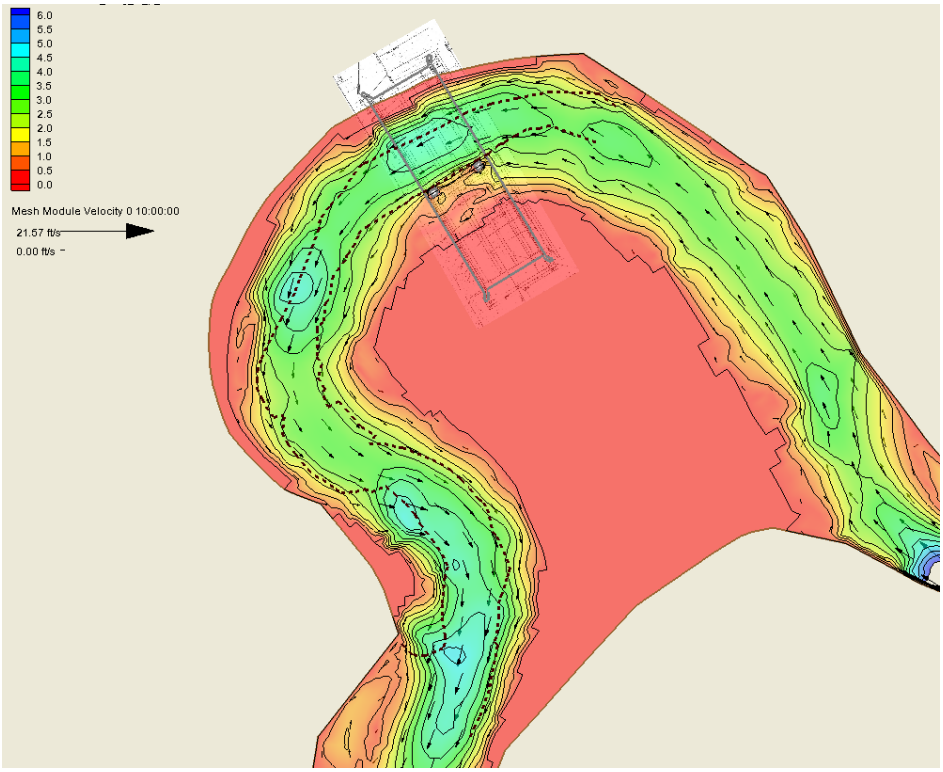

Figure 3 Averaged Depth Contours for the Q100 @ Kings Creek (Br. 36-0054)

The critical velocity criterion was applied to estimate the density of smart rocks given d = 0.25 m and the hydraulic parameters read from Figure 2 and Figure 3. Specifically, V = 2.5 m/s and y = 3.0 m were considered at Bent 2. Again, K_s = 0.052 and $n = 0.041 d^{1/6} = 0.0325$; $S_s = \rho_s/1000$ where ρ_s is the mass density of smart rocks in kg/m^3. The density of smart rocks is estimated by:

$$2.5 = \frac{0.052^{1/2}\left(\frac{\rho_s}{1000} - 1\right)^{1/2} 0.25^{1/2} 3.0^{1/6}}{0.0325}, \quad \rho_s = 1272.6\ kg/m^3$$

In the final design of the smart rock, the size of 0.25 m and density of 1272.6 kg/m^3 will be referenced as the base value.

Task 2.1 Final Design of Smart Rocks

A. Size and Density

In general, the stronger the magnetic field that a smart rock generates in reference to the ambient magnetic field, the higher the accuracy of the smart rock localization. One cylindrical magnet (4" in diameter and 2" in height) was used in the recently completed field mock-up tests for the localization of the magnet by magnetic strength measurement. However, two of them stacked together (4" in diameter and 4" in total height) or one larger magnet (6" in diameter and 2" in height) are considered to improve the effective measurement distance for magnetic field. Two or more magnets stacked together will behave exactly like a single magnet of the combined size. Moreover, the larger a magnetic source, the stronger the magnetic field it generates. The magnetic moment that determines the magnetic field of the magnetic source is directly related to the volume of the magnet(s) and the intensity of magnetization. Therefore, two stacked magnet will be considered as the magnetic core of the smart rock for field deployment.

Due to increasing of the magnet size, the inside and outside balls for the fabrication of an APUS must be increased. In this study, the diameter of the commercially available inside ball to ensure that it always floats is 25 cm and. The diameter of the outside ball is 28cm. These two sizes of balls were recently ordered. The density of the updated smart rock will also be calculated according to the incipient motion equations as did in the second progress report. Similarly, the final size of the smart rock (i.e. the size of the concrete mold) will be firstly determined according to the concrete mold size. The density of the concrete encased smart rock can then be modified to satisfy the critical condition of the incipient motion. Based on commercial availability, the diameter of the concrete sphere mold is initially selected as 14.5".

B. Internal Configuration

The configuration of an updated smart rock with two stacked magnet is based on the gravity balance as schematically shown in Figure 4.

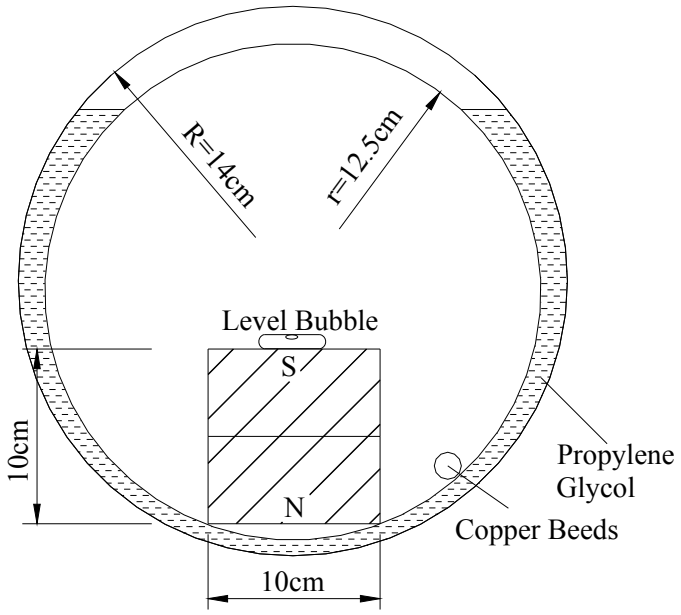

Figure 4 Schematic View of the Updated Smart Rock

Task 3.1 Time- and Event-based Field Measurements - Field Tests Completed & Reported

In this task, a mock-up field test was carried out on the deck of US63 Bridge over the Gasconade River using a smart rock of the APUS model. A modular wood frame was designed and made to support two magnetometer sensors. It was light and easily extended down from the bridge deck to measure the magnetic field intensities at various points. The entire procedure of the field test was planned, practiced, and recorded in order to develop an effective and efficient field test protocol for future tests at bridge sites.

A. Test Setup and Layout

All tests were conducted near the bridge pier at Bent 11 as shown in Figure 5. A total station was set near the abutment on the Rolla side. The center of the total station was used as the origin of a Cartesian coordinate system XYZ with X-, Y-, and Z- axles defined along the longitudinal (along the traffic), transversal and vertical downward directions, respectively. Four locations of smart rocks (APUS), designed by M1, M2, M3 and M4 in Figure 5(a, b), were selected to take into account a combination of horizontal positions and depths in bridge scour monitoring. The magnetometer sensors mounted on the wood frame were extended down from the bridge railing to measure the ambient magnetic field and the magnetic field of the smart rock placed at different points. The wood frame was placed at two positions marked as C1 and C2 on two sides of the pier. For each column, five horizontal lines denoted as L1, L2, L3, L4 and L5 with equal distance of 0.5 m represent five elevations where measurements are taken in Z-direction. Specifically, the magnetic fields of a magnet placed at M1, M2 or M3 were measured at each of the five elevations when the frame is placed at C1 as shown in Figure 5(b). The magnetic field from M1, M2 or M4 was measured at each of the five elevations when the frame is placed at C2 as shown in Figure 5(c). Therefore, the total magnetic field measurement points for each smart

rock at M1, M2, M3 or M4 are 20, 20, 10, and 10 points, respectively. The total station set near the abutment was used to survey the coordinates of four smart rocks and a total of 20 magnetometer sensor positions as ground true data.

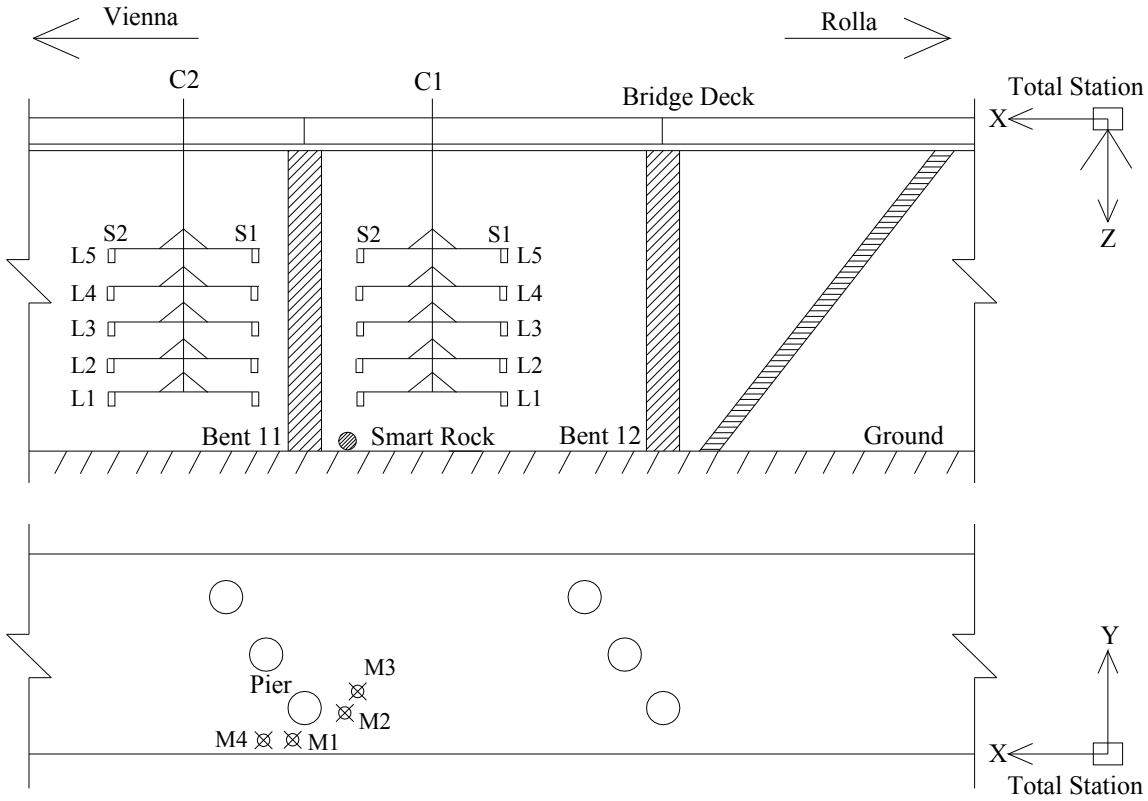

(a) Schematic view of smart rock and sensor locations in plane

(b) Layout of smart rocks and sensor heads at position C1

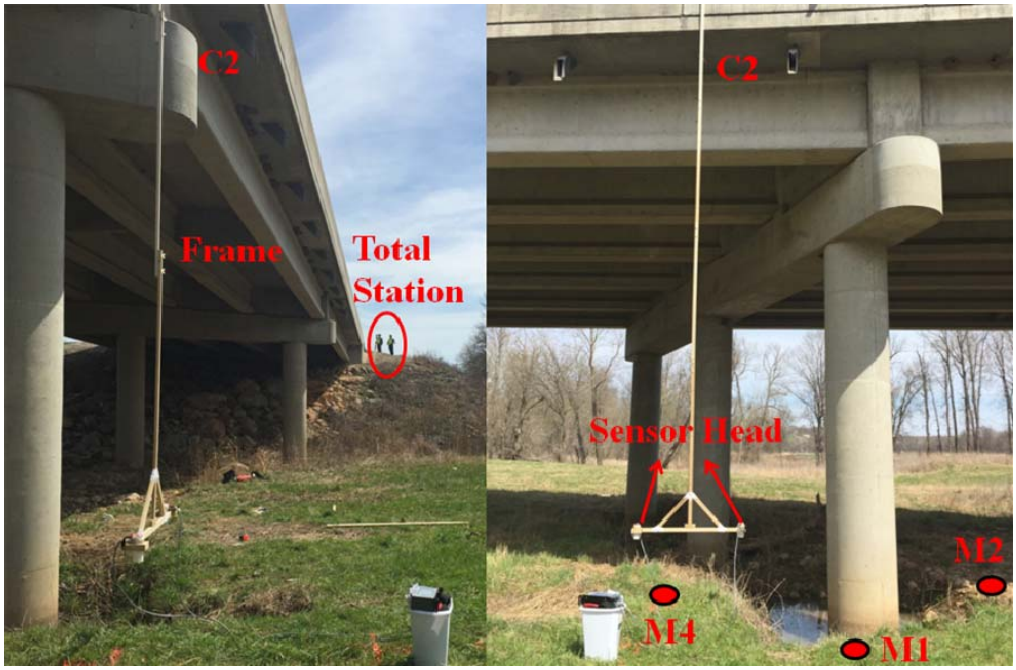

(c) Layout of smart rocks and sensor heads at C2 position

Figure 5 Test Setup at Bridge Site

A. Test Procedures

(1) ***Set the XYZ Coordinate System.*** As shown in Figure 5(c), the total station or the origin of the coordinate system was set up on the side of the bridge approach and on the top of the bridge embankment on the Rolla side in order to view all the measurement points. Select the longitudinal (traffic) direction of the bridge deck as the X-axis. The Y-axis is perpendicular to the X-axis in the horizontal plane. Z-axis was chosen downward according to the right hand rule. The planes OXZ and OXY are shown in Figure 5(a).

(2) ***Assemble the Wood Frame and Mount the Magnetometer Sensor Head.*** Based on the approximate height of 7.5 m from the ground to the bridge railing, up to four equal lengths (2.5 m) of the wood pole were quickly connected with plastic screws. A bolt was used to lock the frame on a horizontal bar supported on the railing and counter weighted by a bucket of sands so that the frame becomes stable. Since the cable length from the sensor head to the console of the magnetometer is only 3 m, the console cannot be operated on the bridge deck; it has to be operated on the ground during the tests. The two sensor heads were attached on the frame based on the ground as shown in Figure 5(b, c).

(3) ***Select the Locations of the Smart Rocks***. As shown in Figures 5(a-c), the smart rocks were located around the bridge pier. Smart rock locations, M1, M2, M3 and M4, were marked by inserting bottle caps into the ground for easy placement of smart rocks on the ground and

convenient measurement of coordinates. The smart rock shown in Figure 6 was placed from point M1 to M4, respectively. A high precision level bubble was used to ensure that the magnet is horizontal.

Figure 6 The Smart Rock in APUS Model

(4) ***Measure the Coordinate of Smart Rocks***. The coordinates of four locations of the smart rock were surveyed by the total station with a prism placed on the APUS at each location.

(5) ***Measure the Coordinate of the Sensor Head and Magnetic Field Intensity of APUS at M1, M2, and M3 When the Frame is Placed at C1***. As shown in Figure 5(a, b), the frame was at the elevation of Level L1 immediately after assembling. Measurements were then taken from L1 to L5. After surveying the coordinate of the two sensor heads at L1 level, the total magnetic field intensity was measured for smart rock located at M1, M2 and M3, respectively. Then, pull up the frame by 0.5 m to Level L2 and measure the coordinate and intensity again for each location. This process continues successively for Level L3, L4, and L5 with 0.5 m spacing.

(6) ***Measure the Coordinate of the Sensor Head and Magnetic Field Intensity of APUS at M1, M2, and M4 When the Frame is Placed at C2***. Move the frame to C2 location at the completion of all measurements at C1 location as shown in Figure 5(a, c). In this case, measurements were taken from L5 to L1 in the reverse order as done at C1 location.

B. Test Results and Discussion

Table 1 summarizes the coordinates of 20 sensor head locations (or measurement points) and 4 smart rock locations in the XYZ coordinate system. For example, the measurement point C1L1S1 means Position C1, Level L1 and Sensor 1 as indicated in Figure 5(a). It is noted that the Y and Z coordinates for the two sensors (S1, S2) at each elevation would be nearly the same if the frame were not deformed or rotated during tests. However, the difference in Y coordinates

of C1L1S1 and C1L1S2 measurements reaches to 0.185 m. This error resulted from the low stiffness of the wood frame and the swing motion caused by the wind. Therefore, a stronger and stiffer frame is needed to reduce the error to a minimum.

Table 1 Coordinates of Smart Rocks and Measurement Points

	X/m	Y/m	Z/m		X/m	Y/m	Z/m
M1	50.963	0.799	7.629	M3	47.297	3.528	7.620
M2	48.021	2.315	7.512	M4	52.607	0.775	7.393
C1L1S1	51.668	0.691	5.746	C2L1S1	51.668	0.691	5.772
C1L1S2	52.797	0.506	5.755	C2L1S2	52.797	0.506	5.770
C1L2S1	47.504	0.709	5.258	C2L2S1	51.650	0.695	5.267
C1L2S2	48.620	0.571	5.267	C2L2S2	52.733	0.560	5.282
C1L3S1	47.436	0.622	4.751	C2L3S1	51.704	0.585	4.775
C1L3S2	48.551	0.477	4.798	C2L3S2	52.791	0.555	4.786
C1L4S1	47.499	0.547	3.948	C2L4S1	51.692	0.553	4.268
C1L4S2	48.606	0.588	3.950	C2L4S2	52.740	0.556	4.259
C1L5S1	47.425	0.551	3.451	C2L5S1	51.675	0.572	3.761
C1L5S2	48.500	0.579	3.449	C2L5S2	52.755	0.570	3.750

The magnetic field intensity at each sensor location was collected when the smart rock was placed at M1, M2, M3 and M4, respectively. Figure 7 shows the magnetic flux density (B) recorded over time at the measurement points C1L1S1 and C1L1S2 with the smart tock placed at M1. It can be seen from Figure 7 that their intensities fluctuated up to 500 nT as a result of the frame motion. Due to the significant fluctuation, the correlation between the measurement point and the magnetic field intensity is weak. The fluctuation would lead to the considerable error in smart rock localization. Therefore, improving the consistency of measured coordinates at each measurement point is a necessity to ensure the accuracy in smart rock localization.

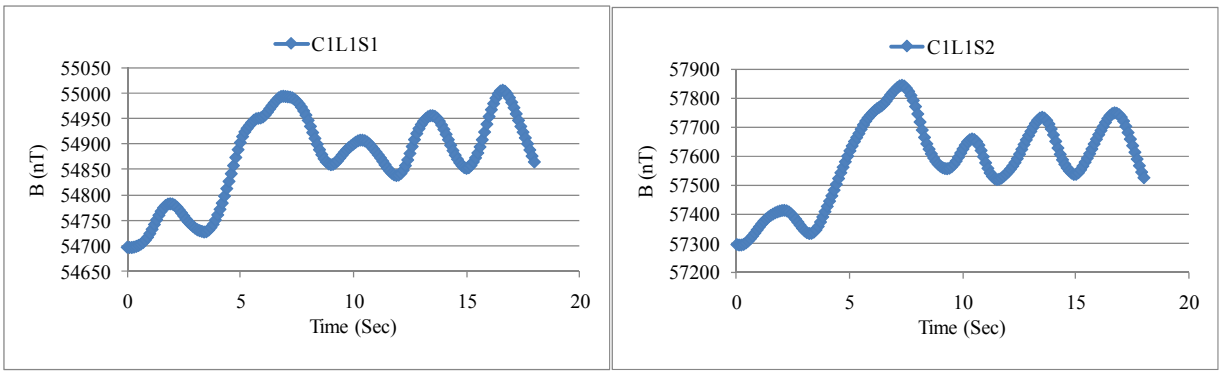

Figure 7 Time-varying Magnetic Field Intensity of C1L1S1 and C1L1S2 for M1

Figure 8 (a, b, c) compares the total intensities of Sensor S1 at Position C1 from Level L1 to L5 for the smart rock placed at M1, M2, and M3, respectively. The lowest Level L1 had the largest intensity because of its proximity to the smart rock. The intensity decreased as the sensor moved

up from L1 to L5. Overall, the level of fluctuation also decreased from Level L1 to L5. Both decreasing trends seem reasonable.

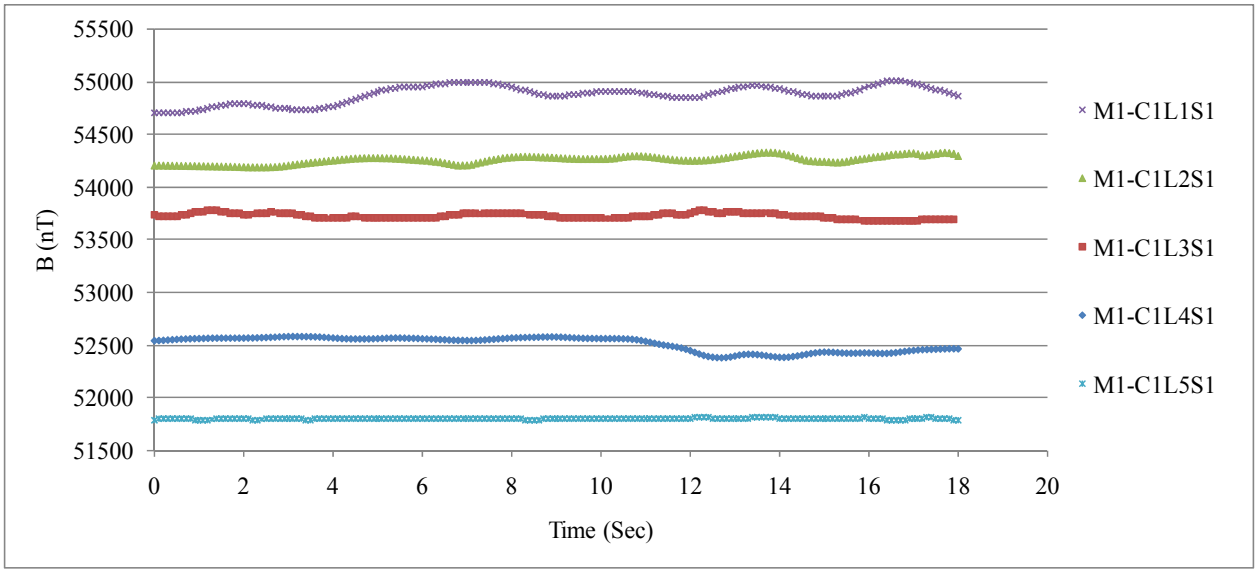

(a) Smart rock at M1

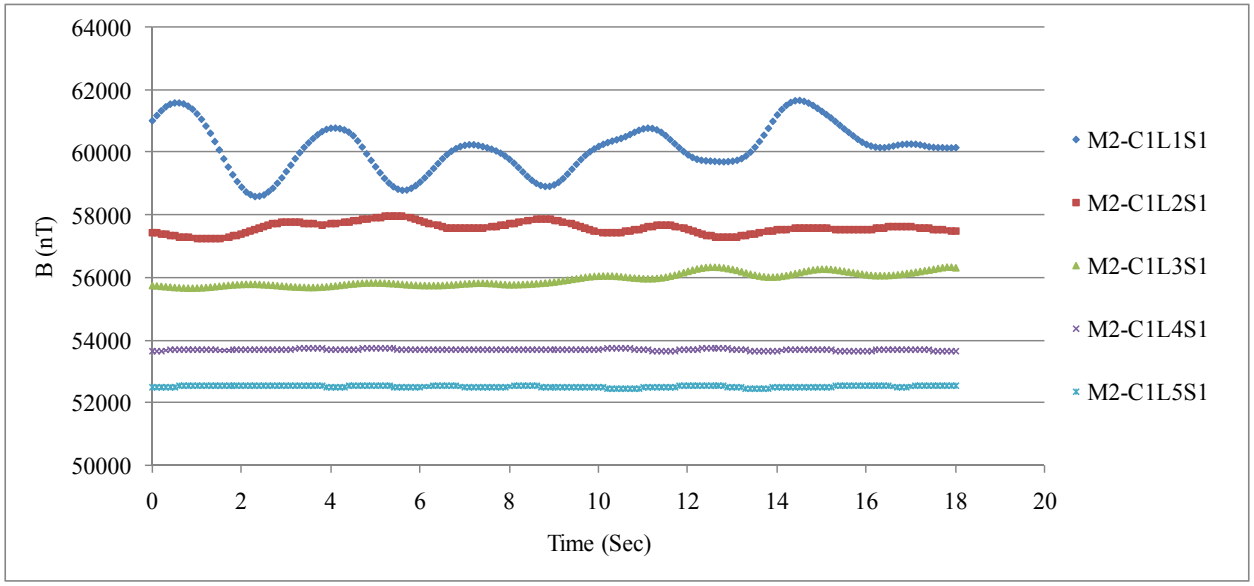

(b) Smart rock at M2

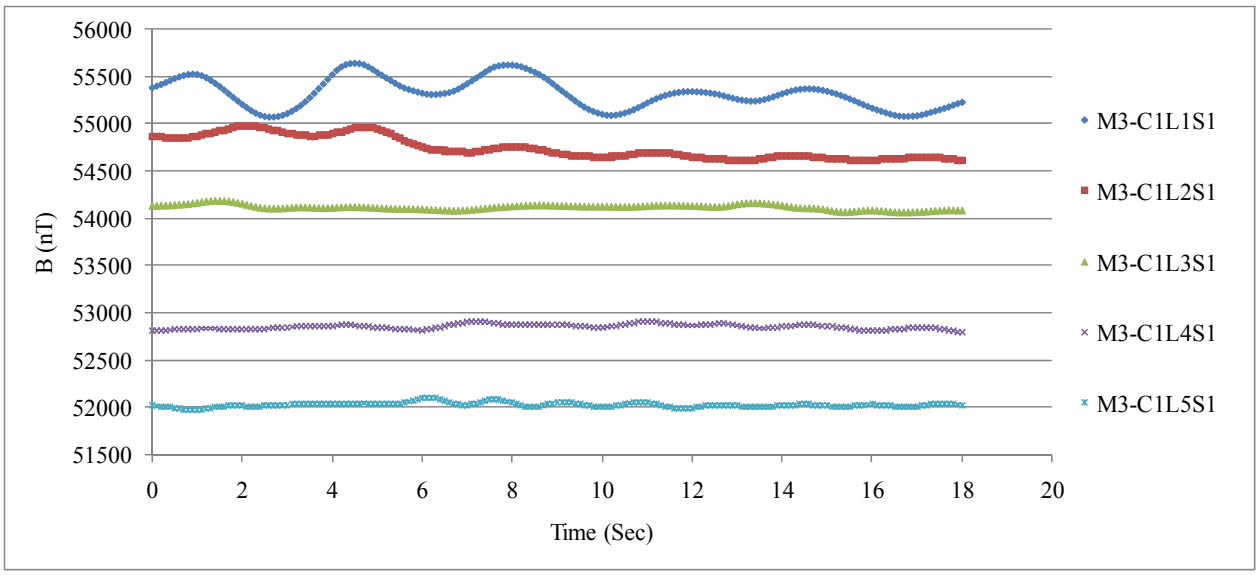

(c) Smart rock at M3

Figure 8 Total Magnetic Field Intensities of Sensor S1 at Position C1 from Level L1 to L5

It can also be observed from Figure 8 that the difference of intensities at Levels L4 and L5 ranged from 500 nT to 1000 nT, which was significant to distinguish the location of the smart rock from that distance. This result indicated that the frame could be further moved up for an effective localization of the smart rock so long as the change in intensity exceeds a minimum of 100nT based on our previous experience. This threshold was mainly determined by the fluctuation of ambient magnetic field or the fluctuation due to slight movement of the sensor head. Therefore, the measurement levels (L1 through L5 to higher locations) should be considered. In addition, the increment of intensity from L1 to higher locations should be monitored during field tests in order to collect useful data efficiently.

In the first progress report (October 1 to December 31, 2014), a localization algorithm was validated with field measurements from the ground. Some of the key data sets required to apply the localization algorithm are three components of the ambient magnetic field due to the effect of the Earth and bridge pier/deck at all measurement points, which was obtained from the specially designed Ambient Magnetic Field Orientation Device (AMFOD). In this report, all measurements are supposed to measure from the bridge deck and the AMFOD is thus not applicable in this case. To use the same localization algorithm, the three components of the ambient magnetic field can alternatively be measured using a three axis magnetometer. Moreover, a direct measurement of the three components of a magnetic field increases the efficiency and accuracy of localization in bridge applications. Equally important, a graphical display capability of the magnetometer would allow a real time check on the quality of measured data during tests at bridge sites.

C. Design of a Rigid yet Light Frame

In the design of a new frame to facilitate field tests, the following factors were taken into account: rigidity, lightweight, ease in installation, rapid assembling, and cost effectiveness. A rigid yet light frame is designed as shown in Figure 9 to minimize the wind-induced disturbance on field measurements. The frame mainly consists of four components (Comp. 1-4) as depicted in Figure 9. Comp.1 is a lower horizontal beam that supports a sensor head for magnetic field intensity measurement and two non-magnetic prisms for the coordinate determination of the sensor. Comp. 2 is a vertical column that allows the access to the measurement points as close to the water surface as possible in field application. Comp. 3 is an upper horizontal beam that functions as an outrigger and support for the column. Comp. 4 is a forklift that allows the three directional movement of the sensor head. Comp.1 will be made of carbon fibers that have a low density of 1800kg/m^3 and high stiffness of 240 GPa compared to other non-magnetic materials. Comp. 2 will be made of modular carbon fiber tubes (1 m in length) that are designed to minimize flexural deformation and resist potential vibration caused by the wind load. The standard tubes can be connected to any required length in field application. Comp. 3 will be made of aluminum alloy with a density of 2700-2810 kg/m^3 and stiffness of 71 GPa. A balanced weight will be applied to ensure that the Comp.3 remains horizontal during tests. All the components can be rapidly assembled at a test site. The forklift is considered to be operated manually in this study but could be operated automatically from a remote site if needed.

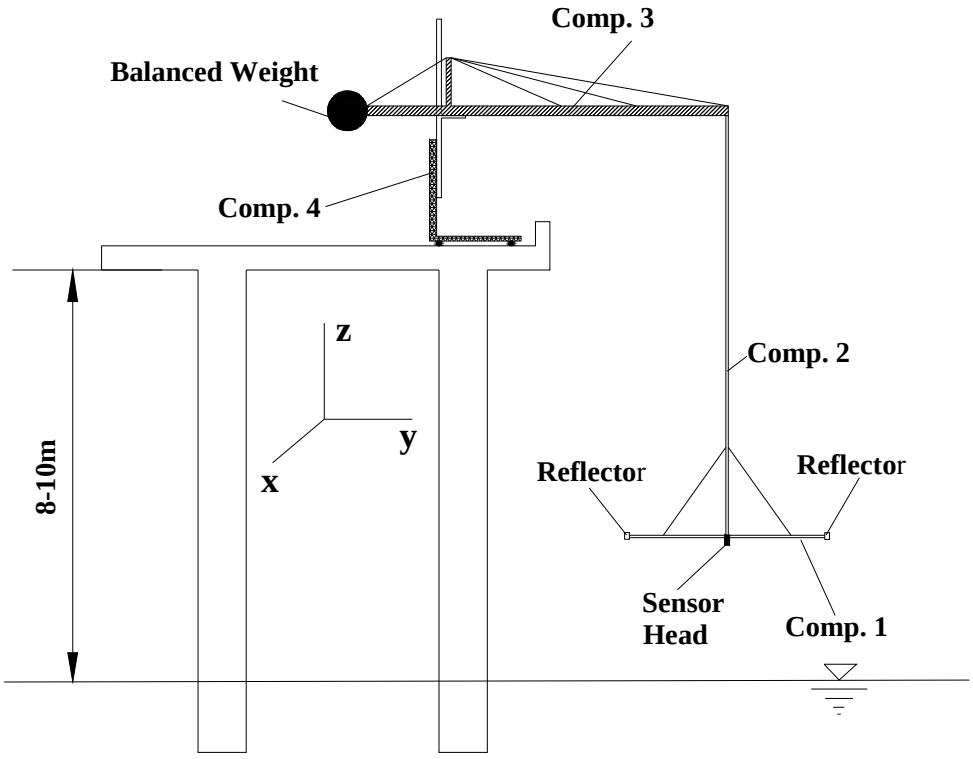

Figure 9 A Rigid yet Light Frame for Field Tests

D. The Three Axis Flux Magnetometer

A digital 3-axes magnetometer system as shown in Figure 10, manufactured by STL Systemtechnik Ludwig GmBH in Konstanz, Germany, has been ordered for this study. It is composed of a digital sensor DM050, a three-channel coax Ethernet hub, a 50 meter coax cable for power and data transmission, and a notebook with STL GradMag software installed for full controlling of measurement, data acquisition and graphical display. The DM050 is a precision magnetometer with 0.002nT resolution, less than 0.06nT/√Hz noise and a field range of ±1mT. It measures the 3 orthogonal field components at a maximum sample rate of 10 kHz. The software also offers the total field as an extra virtual channel. Typical sources of errors due to axis misalignment, scaling, offset and phase are eliminated to the greatest extent possible with a digital signal conditioning strategy. The software offering full control over all system features, real-time monitoring of data and data documentation greatly improves the efficiency of field data analysis and display.

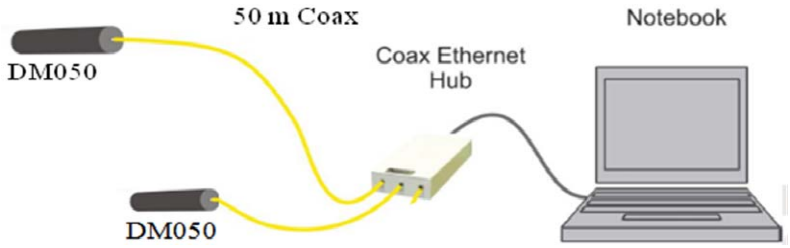

Figure 10 The Digital Three-axis Flux Magnetometer System

E. Deployment Plan of Smart Rocks

A general deployment plan of smart rocks was developed for four bridge sites and depicted in Figure 11(a, b, c, d). Two smart rocks will be placed on the two sides of the front pier of Bent 4 for the US63 Bridge over the Gasconade River since the bridge scour is generally formed along two sides of the pier in the upstream. Similarly, two smart rocks will be deployed around the front pier of Bent 7 for the I-44 Bridge over the Roubidoux Creek. Four smart rocks will be deployed at the US1 Waddell creek bridge, two of them for the riprap monitoring around abutment 1 and the other two for the scour around the front pier of Bent 2. Finally, for the US9 Kings creek bridge, two smart rocks will be placed at the main flow side of the front and back pier for Bent 2 to monitor the scour around the two piers. The exact locations of the smart rocks will be determined when deployed.

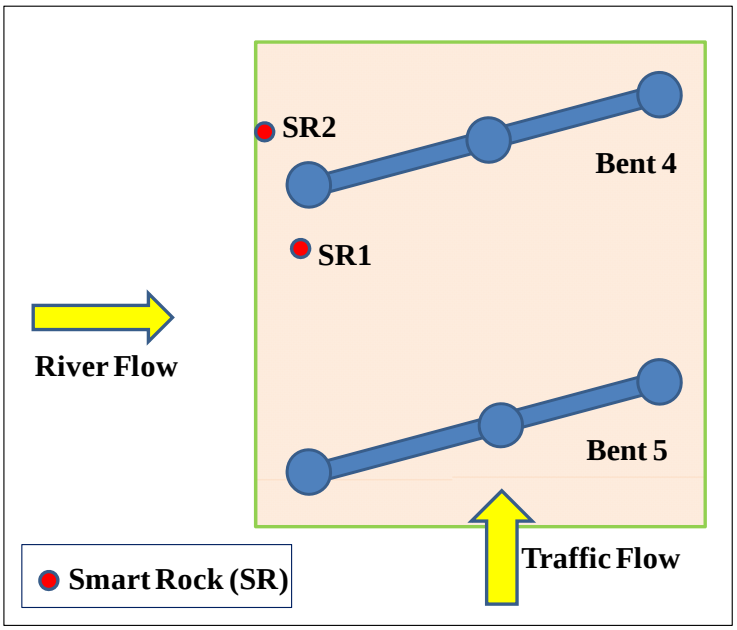

(a) US63 Gasconade River Bridge

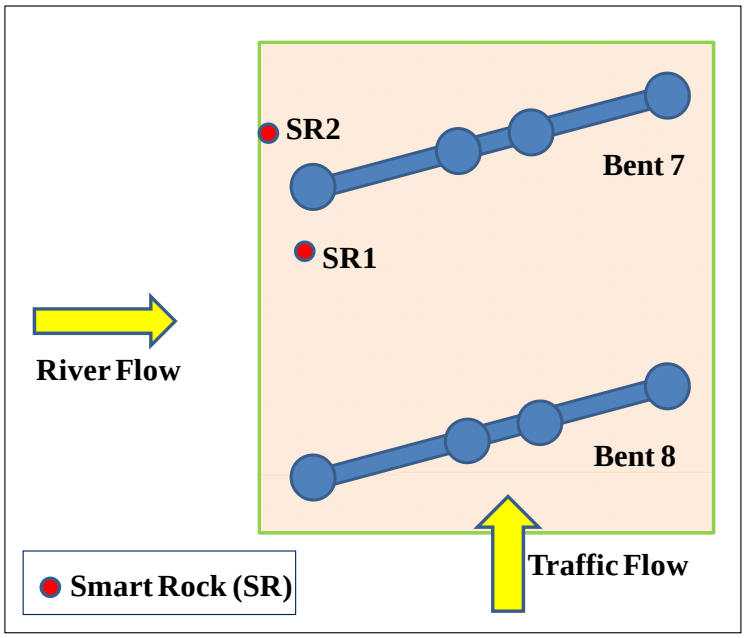

(b) I44 Roubidoux Creek Bridge

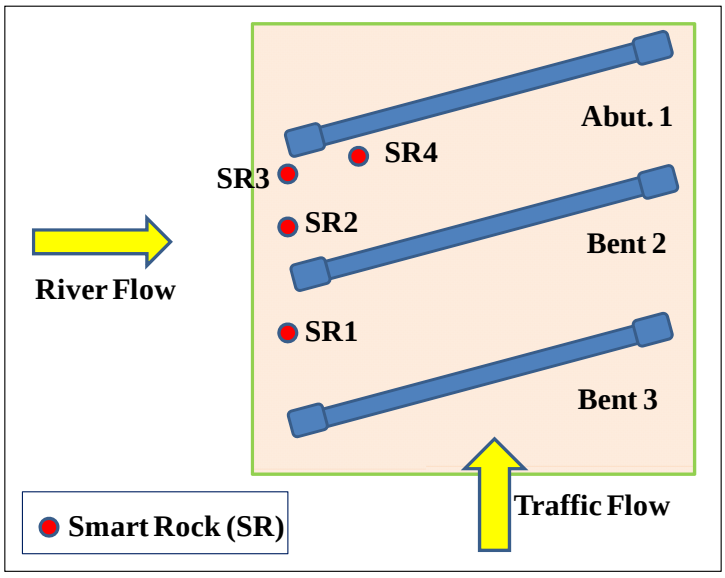

(c) HYW1 Waddell Creek Bridge

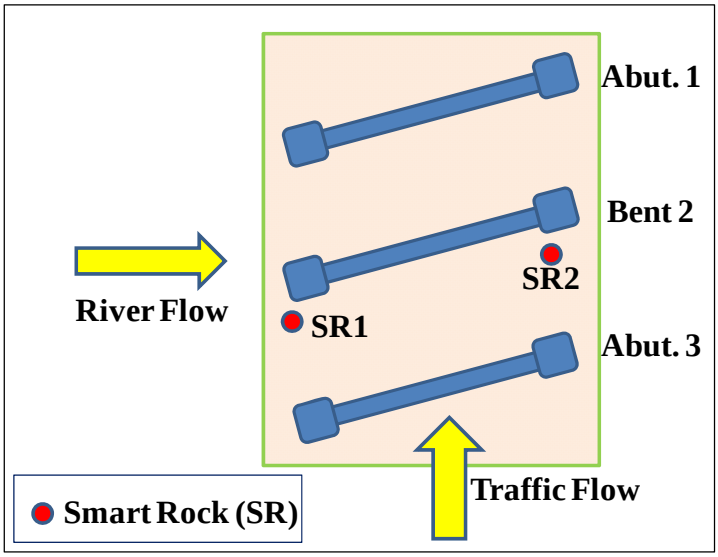

(d) HYW 9 Kings Creek Bridge

Figure 11 Smart Rock Deployment Plan

Task 3.2 Visualization Tools for Rock Location Mapping over Time - Software Completed & Tested

This task will not start till the 5th quarter.

Task 4 Technology Transfer, Report and Travel Requirements - Quarterly Report Submitted, Travel Completed, or Meeting Conducted

The 3st quarterly report is being submitted.

I.2 PROBLEMS ENCOUNTERED

In this quarter, smart rock deployment was postponed due to the need for a redesign of the rigid yet light frame and for a 3-axis magnetometer for effective localization of smart rocks.

I.3 FUTURE PLAN

The following task and subtasks will be executed during the next quarter.

Tasks 2.2 Prototyping of Passive Smart Rocks - Concrete Encasement Cast

Based on the final design of smart rocks, concrete encasement will be cast for final deployment at four bridge sites.

Task 3.1 Time- and Event-based Field Measurements - Field Tests Completed & Reported

The field tests at four bridge sites will be conducted to validate the localization of smart rocks.

Task 3.2 Visualization Tools for Rock Location Mapping over Time - Software Completed & Tested

This task will not start till the 5th quarter.

Task 4 Technology Transfer, Report and Travel Requirements - Quarterly Report Submitted, Travel Completed, or Meeting Conducted

The 4th quarterly report will be prepared and submitted.

.

II – BUSINESS STATUS

II.1 HOURS/EFFORT EXPENDED

The planned hours and the actual hours spent on this project are given and compared in Table 2. In the third quarter, the actual hours are less than the planned hours, leading to an actual cumulative hour of approximately 31% of the planned hours. The cumulative hours spent on various tasks by personnel are presented in Figure 12.

Table 2 Hours Spent on This Project

	Planned		Actual	
	Labor Hours	Cumulative	Labor Hours	Cumulative
Quarter 1	945	945	176	176
Quarter 2	752	1697	294	471
Quarter 3	752	2449	294	765
Quarter 4				
Quarter 5				
Quarter 6				
Quarter 7				
Quarter 8				

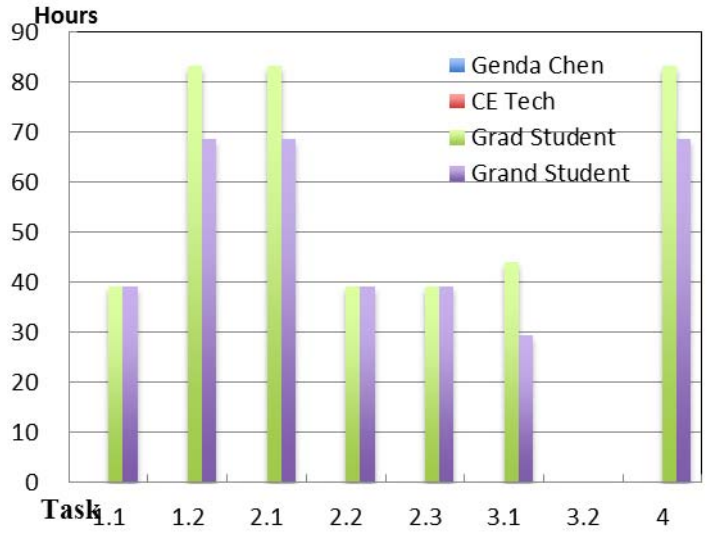

Figure 12 Cummulative Hours Spent on Various Tasks by Personnel

II.2 FUNDS EXPENDED AND COST SHARE

The budgeted and expended OST-R funds accumulated by quarter are compared in Figure 13. Approximately 61% of the budget has been spent till the end of third quarter. The actual cumulative expenditures from OST-R and MS&T/MoDOT are compared in Figure 14. The expenditure from OST-R ($63,301) is less than the combined amount from the MS&T and MoDOT ($77,740).

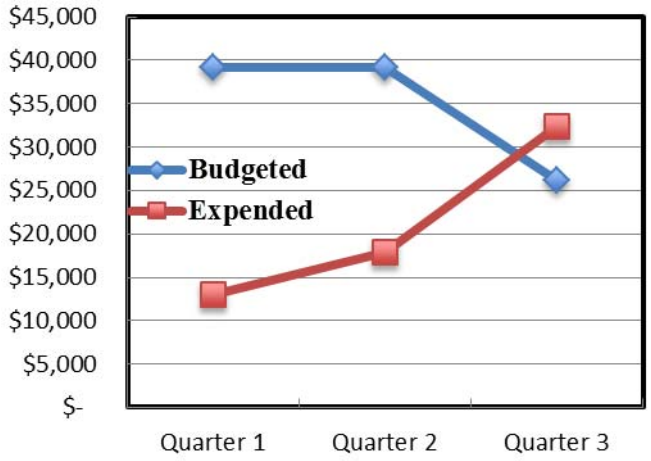

Figure 13 Comparison of OST-RBudget and Expenditure Accumulated by Quarter

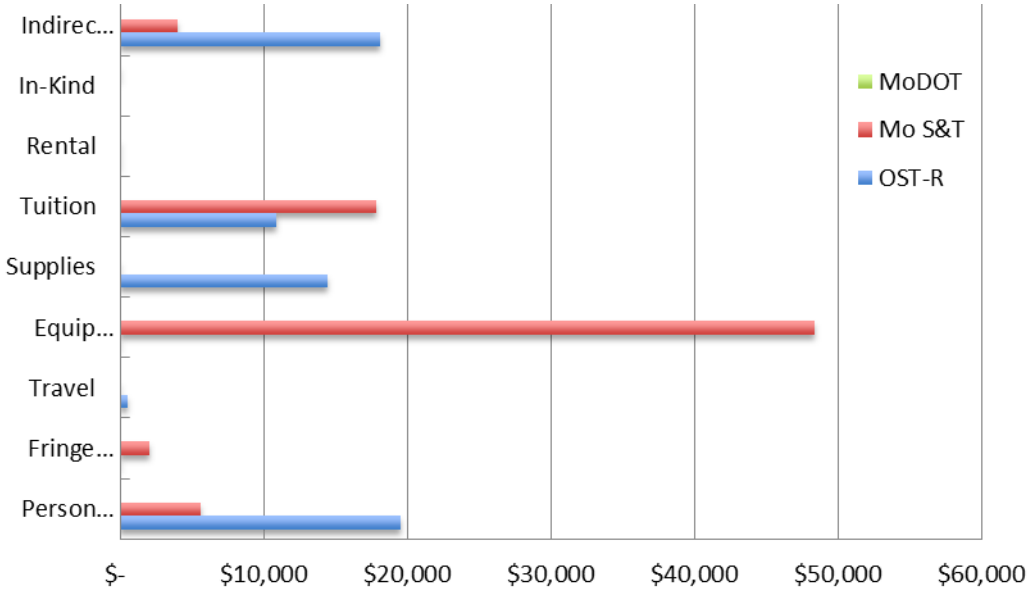

Figure 14 Cummulative Expenditures by Sponsor